Journal of Physics: Conference Series **547** (2014) 012045 doi:10.1088/1742-6596/547/1/012045

A simplified analytical model of radiative heat transfer in open cell foams

A Andreozzi[1], **N Bianco**[1], **S Cunsolo**[1], **V Naso**[1] **and M Oliviero**[2]
[1] Dipartimento di Ingegneria Industriale, Università degli studi Federico II, 80 P.le Tecchio, 80125, Napoli, Italy
[2] Istituto per i materiali compositi e biomedici, Consiglio Nazionale delle Ricerche, 1 P.le Fermi, 80055, Portici (Napoli), Italy

E-mail: nicola.bianco@unina.it

Abstract. A simplified one-dimensional analytical model of radiative heat transfer in foams is presented, based on the idea of dividing the porous material into layers at the pore level and then modeling each layer of the porous material as an equivalent semi-transparent, absorbing and reflecting plane. Compared to existing models, the model proposed in this paper has the advantage of explicitly accounting for the geometry of the foam and the radiative energy fluxes, at the same time ensuring self-consistency and offering the computational lightness of analytical models, without sacrificing the mathematical simplicity of the formulation. Using a regular cubic lattice representation and assuming diffuse radiation, straightforward analytical correlations are derived to evaluate the characteristics both of single layers of foam and of finite thickness samples, accounting for various boundary conditions. The predictions of the model are in good agreement with experimental data taken from the literature.

1. Introduction

Open cell metal and ceramic foams are being widely adopted in many heat transfer areas, such as compact heat exchangers, fire barriers and volumetric absorbers in concentrating solar systems receivers. In many heat transfer applications thermal radiation is the predominant heat transfer mode in open cell solid foams [1].

Radiative behavior of open cell foams has been investigated using analytical, numerical and experimental methods [2].

Most analytical models in literature are based on independent scattering in randomly dispersed media in geometric optics regime. The foam is modeled as a random dispersion of particles, whose contributions are summed up to obtain the effective radiative properties. This approach, originally proposed by Glicksmann et al. [3], who modeled the foam as a set of dodecahedral cells, was also followed by Kuhn et al. [4-5], and Doermann and Sacadura [6]. Coquard and Baillis [7], Coquard et al. [8], and Loretz et al. [9] extended these results by considering models with different cell and strut shapes.

Some alternative approaches have been attempted by a number of authors. Kamiuto [10] calculated radiative properties of the foam on the basis of Mie scattering theory. De Micco and Aldao [11] proposed a model based on treating the foam as a series of high-optical density and low-optical density layers. The model of Zhao et al. [12] is one of the very few that try to explicitly account for the cell

organization of the foam, though using a simplified cubic lattice. Contento et al. [13] modified the model proposed in [12] in order to improve its accuracy.

In this paper, following an approach similar to that used by Zhao et al. [12], an alternative analytical model is proposed. Compared to existing models, the model proposed in this paper has the advantage of explicitly accounting for the geometry of the foam and the radiative energy fluxes, at the same time ensuring self-consistency and offering the computational lightness of analytical models, without sacrificing the mathematical simplicity of the formulation. Some applications are shown and, finally, a comparison of predictions with experimental data taken from the literature is made.

2. Model and analysis

As a premise, it is worth summing up the assumptions made in the formulation of the model:

- surface reflectivity independent of wavelength and incidence angle;
- geometric optics approximation;
- diffuse reflection;
- the foam is modeled as a uniform cubic lattice;
- the model is one-dimensional.

2.1 Idealized cell structure

The microstructure of ideal open celled foams is constituted by cells with 12-14 square, pentagonal and hexagonal faces. In the present study reference is made to the simplified cubic representation proposed by Bhattacharya et al. [14]. The structure is depicted in figure 1.

Unit cells are characterized by the cell diameter, d_p, and the ligament diameter, d_0, that can be correlated with the characteristic parameters of foams, such as porosity, φ, and pores per inch, *PPI*.

In order to ensure an unchanged porosity in the simplified cubic representation, the following correlation has to hold

$$d_0 \approx 2\left(\frac{1-\varphi}{3\pi}\right)^{1/2} d_p \tag{1}$$

Additionally, the cell diameter is chosen so that the cubic cells have the same average diameter as the real cells. This can be achieved by using directly measured values of the cell diameter or, alternatively, when only technical specifications are available, the following approximate correlation can be used

$$d_p \approx 25.4\ (PPI)^{-1}\ [mm] \tag{2}$$

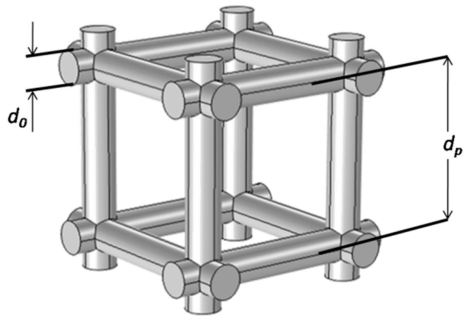

Figure 1. Structure of an open celled foam.

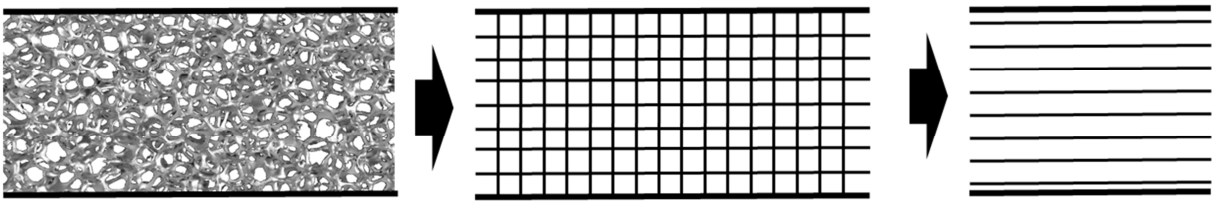

Figure 2. Partition of the cubic lattice into parallel planes.

2.2 Equivalent planes

After simplifying the original foam structure the assumed cubic lattice can be partitioned into parallel planes, each of them corresponding to a layer of cubes, by means of the process sketched in figure 2.

Reference being made to an indefinite single layer of cells, the top and bottom planes, along with the enclosed solid matter, constitute an optical cavity, as depicted in figure 3.

The optical cavity can now be used to calculate the equivalent characteristics of the plane. The view factor, F_{12}, between the opposite planes 1 and 2 can be evaluated once the view factors between the opposite faces A and B, F_{AB}, and between the contiguous orthogonal faces A and C, F_{AC}, are known. To this aim, one can first notice that the view factor between the two planes is equal to the view factor between a single face and the opposite plane, which can be calculated considering both direct radiation and radiation through side faces.

In all practical foams geometry F_{AB} and F_{AC} assume a nearly common value, given by the following correlation [15]

$$F_{AB} \approx F_{AC} \approx \frac{2}{\pi X^2}\left[\ln\left(\frac{(1+X^2)^2}{1+2X^2}\right)^{1/2} + 2X(1+X^2)^{1/2}\tan^{-1}\left[X(1+X^2)^{-1/2}\right] - 2X\tan^{-1}X\right] \quad (3)$$

where $X = 1 - d_0/d_p$.

It is also worth noticing that equation (3) can be approximated as

$$F_{AB} \approx F_{AC} \approx 0.26\,X - 0.063 \quad (4)$$

for all typical X values of open cell solid foams.

Equation (4) allows to evaluate F_{12}, F_{S1}, F_{1S} and F_{SS}, by making use of reciprocity and cavity properties

$$F_{12} = F_{AB} + 8\,F_{AB}^2\ \ (1 - 3F_{AB})^{-1} \quad (5)$$

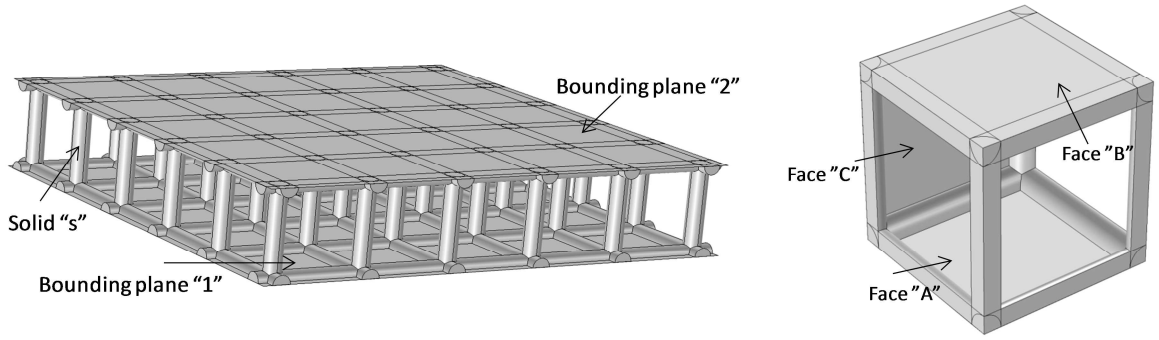

Figure 3. Sketch of the optical cavity.

$$F_{1S} = 1 - F_{12} \tag{6}$$

$$F_{S1} = F_{1S}(A_1/A_S) \tag{7}$$

$$F_{SS} = 1 - 2\,F_{S1} \tag{8}$$

The characteristics of a plane optically equivalent to the cell layer considered can then be determined from the amount of emitted, reflected and transmitted radiation. The solid surface is considered as an opaque grey body, characterized by emissivity ε and reflectivity $\rho = 1 - \varepsilon$. Reflection is assumed to be diffuse and multiple reflection effects are taken into account.

The plane is characterized in terms of equivalent emissivity, ε_{eq}, reflectivity, ρ_{eq}, and transmissivity, τ_{eq}. The following correlations are obtained

$$\varepsilon_{eq} = \varepsilon\,F_{1S}(1 - \rho\,F_{SS})^{-1} \tag{9}$$

$$\rho_{eq} = \rho\,F_{1S}\,F_{S1}(1 - \rho\,F_{SS})^{-1} \tag{10}$$

$$\tau_{eq} = F_{12} + \rho_{eq} \tag{11}$$

2.3 Plane grouping

Using the aforementioned correlations, any given thickness of foam can be treated as a series of planes with given optical properties. In some applications, it can be useful to introduce a further simplification and determine a single plane optically equivalent to a group of *n* contiguous planes. This is accomplished by using recursive relations for the emissivity, ε_p^n, reflectivity, ρ_p^n, and transmissivity, τ_p^n, which are hereby presented

$$\varepsilon_p^n = \varepsilon_{eq} + \varepsilon_{eq}\left[\tau_{eq}\,\rho_p^{n-1}\left(1 - \rho_{eq}\,\rho_p^{n-1}\right)^{-1}\right] + \varepsilon_p^{n-1}\left[\tau_{eq}\left(1 - \rho_{eq}\,\rho_p^{n-1}\right)^{-1}\right] \tag{12}$$

$$\rho_p^n = \rho_{eq} + \tau_{eq}^2\,\rho_p^{n-1}\left(1 - \rho_{eq}\,\rho_p^{n-1}\right)^{-1} \tag{13}$$

$$\tau_p^n = \tau_p^{n-1}\,\tau_{eq}\left(1 - \rho_{eq}\,\rho_p^{n-1}\right)^{-1} \tag{14}$$

It should be remarked that the values of $\varepsilon_p^{\,0}$, $\rho_p^{\,0}$ and $\tau_p^{\,0}$ should be chosen such as to fit the effective boundary condition. For example, if the boundary is a flat metal plate, its emissivity and reflectivity can be set equal to $\varepsilon_p^{\,0}$ and $\rho_p^{\,0}$, whereas if the boundary is an open surface $\tau_p^{\,0}$ should be set equal to 1.

The three successions are convergent and the values $\varepsilon_p^{\,\infty}$, $\rho_p^{\,\infty}$ and $\tau_p^{\,\infty}$ depend only on ε_{eq}, ρ_{eq} and τ_{eq}, i.e. the optical characteristics of a sufficiently thick foam sample depend only on the characteristics of the foam. The above characteristics can be obtained either by iteration or using the following correlations

$$\varepsilon_p^{\infty} = \varepsilon_{eq}\left\{\left[1 + \rho_p^{\infty}(\tau_{eq} - \rho_{eq})\right]\left(1 - \rho_{eq}\,\rho_p^{\infty} - \tau_{eq}\right)^{-1}\right\} \tag{15}$$

$$\rho_p^{\infty} = \left\{1 + \rho_{eq}^2 - \tau_{eq}^2 - \left[\left(1 + \rho_{eq}^2 - \tau_{eq}^2\right)^2 - 4\,\rho_{eq}^2\right]^{1/2}\right\}\left(2\,\rho_{eq}\right)^{-1} \tag{16}$$

$$\tau_p^{\infty} = 0 \tag{17}$$

2.4 Two flux model

A simple two-flux model [15] can be now implemented to manage radiation in the layered structure (figure 4).

Since, in the following, correlations will be given in the form of reverse recurrences, a reverse form of equations (12 - 14) is presented

$$\varepsilon_p^n = \varepsilon_{eq} + \varepsilon_{eq}\left[\tau_{eq}\,\rho_p^{n+1}\left(1-\rho_{eq}\,\rho_p^{n+1}\right)^{-1}\right] + \varepsilon_p^{n-1}\left[\tau_{eq}\left(1-\rho_{eq}\,\rho_p^{n+1}\right)^{-1}\right] \tag{18}$$

$$\rho_p^n = \rho_{eq} + \left[\tau_{eq}^2\,\rho_p^{n+1}\left(1-\rho_{eq}\,\rho_p^{n+1}\right)^{-1}\right] \tag{19}$$

$$\tau_p^n = \tau_p^{n+1}\left[\tau_{eq}\left(1-\rho_{eq}\,\rho_p^{n+1}\right)^{-1}\right] \tag{20}$$

As it is shown in figure 4, the calculation of radiosities J_y and J_{-y} is performed considering three contributions:

a. the heat flux irradiated from the plane in the chosen direction;
b. the heat flux irradiated from the plane in the opposite direction and reflected by the boundary plane;
c. the heat flux irradiated from the rest of the domain in the chosen direction that passes through the boundary plane.

The radiosity J_y can be written as

$$J_y = \varepsilon_{eq}\,\sigma\,T^4 + \varepsilon_{eq}\left[\tau_{eq}\,\rho_{p,y}^0\left(1-\rho_{eq}\,\rho_{p,y}^0\right)^{-1}\right]\sigma\,T^4 + J_y'\left[\tau_{eq}\left(1-\rho_{eq}\,\rho_{p,y}^0\right)^{-1}\right] \tag{21}$$

It is worth noticing that equation (21) can be easily generalized in the form of a reverse recursion. Then the equations for the calculation of the radiosities in both directions can be written as

$$J_y^n = \varepsilon_{eq}\,\sigma\,T_n^4 + \varepsilon_{eq}\left[\tau_{eq}\,\rho_{p,y}^n\left(1-\rho_{eq}\,\rho_{p,y}^n\right)^{-1}\right]\sigma\,T_n^4 + J_y^{n+1}\left[\tau_{eq}\left(1-\rho_{eq}\,\rho_{p,y}^n\right)^{-1}\right] \tag{22}$$

$$J_{-y}^m = \varepsilon_{eq}\,\sigma\,T_m^4 + \varepsilon_{eq}\left[\tau_{eq}\,\rho_{p-y}^m\left(1-\rho_{eq}\,\rho_{p,-y}^m\right)^{-1}\right]\sigma\,T_m^4 + J_{-y}^{m+1}\left[\tau_{eq}\left(1-\rho_{eq}\,\rho_{p,-y}^m\right)^{-1}\right] \tag{23}$$

where J_y^N and J_{-y}^M are the first elements of the recursion and are chosen to represent the irradiation coming from boundary planes. For opaque plates with emissivity $\varepsilon_p{}^N$ and $\varepsilon_p{}^M$, J_y^N and J_{-y}^M are equal to

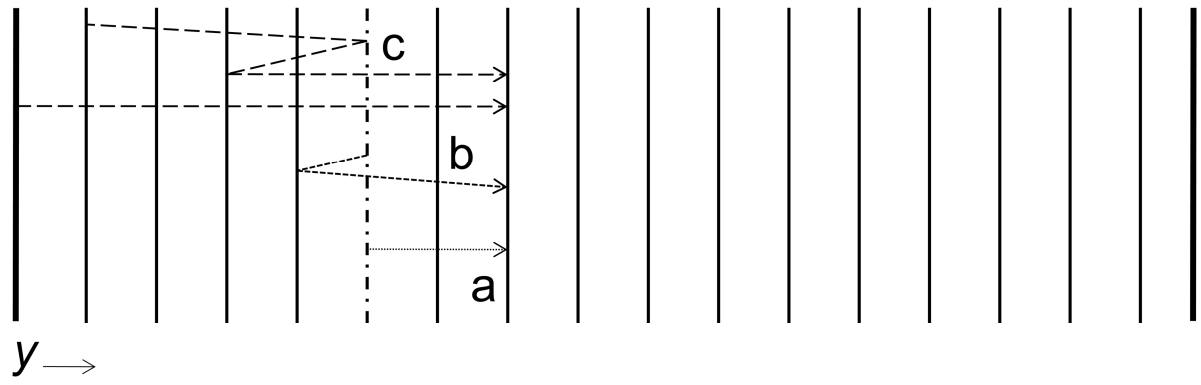

Figure 4. Schematic illustration of contributions to radiosities.

$$J_y^N = \varepsilon_p^N \, \sigma \, T_N^4 \tag{24}$$

$$J_{-y}^M = \varepsilon_p^M \, \sigma \, T_M^4 \tag{25}$$

For an open boundary with the irradiations $I_0{}^N$ and $I_0{}^M$ one can simply write

$$J_y^N = I_0^N \tag{26}$$

$$J_{-y}^M = I_0^M \tag{27}$$

One can remark that the recursions can be truncated, giving approximated solutions. It has been found that a 10 term approximation gives accurate results, with an error less than 5%, in most practical cases.

Finally the net radiative heat flux, q_r, can be determined, taking into account reflection effects, using the following correlation

$$q_r = \left[J_y^0\left(1-\rho_{p,-y}^0\right) - J_{-y}^0(1-\rho_{p,y}^0)\right]\left(1-\rho_{p,y}^0\,\rho_{p,-y}^0\right)^{-1} \tag{28}$$

3. Applications

In the following some applications of the model to problems commonly found in literature will be presented, along with some useful simplifications.

3.1 Evaluation of the radiative conductivity

The equations presented in the previous section can be used to predict the radiative conductivity, k_r, on the basis of a linear, one-dimensional modeling of the phenomenon. The radiative conductivity is currently used when account is to be taken of the radiation effects [1].

A uniform and linear thermal gradient dT/dy is imposed on the foam, which takes the form of a constant ΔT = dT/dy (d_p) between contiguous planes, and then k_r is written as

$$k_r = q_r(\mathrm{d}T/\mathrm{d}y)^{-1} \tag{29}$$

If the foam material can be considered black and the boundary effects can be neglected (N > 20, M > 20), equations (22), (23) and (28) greatly simplify, and an approximate analytical solution can be derived

$$k_r = 4\, d_p \frac{1+\tau_{eq}}{1-\tau_{eq}}\, \sigma\, T^3 \tag{30}$$

A numerical study has been carried out, which showed that emissivity has minor effects on predicted radiative conductivity, down to very low values (ε < 0.05). Therefore, equation (30) can be used for the determination of k_r in thick foam samples.

3.2 Simplified treatment of external sources of radiation

In some cases (for example, in volumetric solar receivers) internal energy transfer may be negligible compared to the heat transfer with an external source. For the sake of simplicity, a domain indefinitely extending in one direction can be considered.

In this case the net incoming radiative heat flux across the n planes can be calculated as

$$q_r^n = I_0\left[\tau_p^n(1-\rho_p^\infty)\right]\left(1-\rho_p^n\,\rho_p^\infty\right)^{-1} \tag{31}$$

with $\tau_p^{\,0} = 1$ and $\rho_p^{\,0} = 0$.

The radiative heat flux absorbed by the solid contained in the *n*th plane, q_{in}^n, is

$$q_{in}^n = q_r^n - q_r^{n+1} \tag{32}$$

Then, the amount of heat flux radiating from plane *n* and irradiating outside of the foam, q_{out}^n, can be calculated as

$$q_{out}^n = \tau_p^n\left[1+\ \tau_{eq}\,\rho_p^\infty\left(1-\rho_{eq}\,\rho_p^\infty\right)^{-1}\right]\left(1-\rho_p^n\,\rho_p^\infty\right)^{-1}\varepsilon_{eq}\,\sigma\,T^4 \tag{33}$$

Finally, the difference between the incoming and the outgoing heat flux gives the net absorbed heat flux

$$q_{net}^n = q_{in}^n - q_{out}^n \tag{34}$$

This term can be easily rewritten as a volumetric internal energy generation term in the energy equation

$$S_r^n = (q_{in}^n - q_{out}^n)\left(d_p\right)^{-1} \tag{35}$$

3.3 Characterization as optically thick media

To obtain the extinction, β, absorption, κ, and scattering, σ_s, coefficients from the model proposed in the present paper, the above correlations developed for the evaluation of the radiative conductivity, k_r, are coupled with the well known Rosseland approximation to obtain the radiative conductivity [1].

Under the Rosseland approximation we can write

$$k_r = [16\,(3\,\beta_R)^{-1}]\,\sigma\,T^3 \tag{36}$$

where β_R is the Rosseland extinction coefficient. Coupling equation (36) with equation (30) we obtain

$$\beta_R = 4\left(1-\tau_{eq}\right)\left[3d_p\left(1+\tau_{eq}\right)\right]^{-1} \tag{37}$$

Under the assumption of grey and diffuse surfaces, one can finally write

$$\beta = \beta_R \tag{38}$$

$$\kappa = (1-\rho)\beta \tag{39}$$

$$\sigma_s = \rho\,\beta \tag{40}$$

4. Validation of the model

The model was validated by comparing its predictions with experimental data of radiative conductivity presented by Zhao et al. [16]. Experimental data presented in [16] was used to set boundary conditions of the problem. The small thickness (30 mm) of the samples used suggests that effects of the boundaries may be not negligible. The nickel coated copper plates enclosing the samples were modeled as gray flat plates with an emissivity ε_b = 0.05. Data on the microscopic features of the

materials was taken from another work from Zhao et al. [17], where SEM imaging was used to accurately characterize the significant process parameters.

The average radiative conductivity, $k_{r,\ av}$, was calculated by simulating coupled conductive-radiative heat transfer in ANSYS Fluent.

The values predicted by the herein proposed model and the experimental data of the radiative conductivity as a function of the temperature, for different values of the Pore Per Inch and the porosity, are reported in figure 5. The figure shows that the model well predicts the temperature dependence of the radiative conductivity exhibited by experimental data. The agreement is rather good, with maximum deviations about 25%.

It may be interesting to focus the attention on a peculiar phenomenon that emerged analyzing data from Zhao et al. [16]. We noticed that for small thicknesses of the foam samples, the effect of boundary emissivity on the value of radiative conductivity averaged along the sample thickness is quite large. The average radiative conductive as a function of boundary emissivity, at 750 K, for a 30 mm thick sample, *30 PPI*, for 90% and 95% porosities, is reported in fig.6. The aforementioned effect is more marked for the higher porosity foam. At very low emissivities of the boundary the 90% porosity foam shows higher average radiative conductivity, as depicted in fig. 6. This is likely caused by high boundary reflectivity "bottlenecking" radiation heat transfer at the boundary, causing energy to be transferred conductively: less porous foams are then advantaged due to their significantly higher effective solid conductivity.

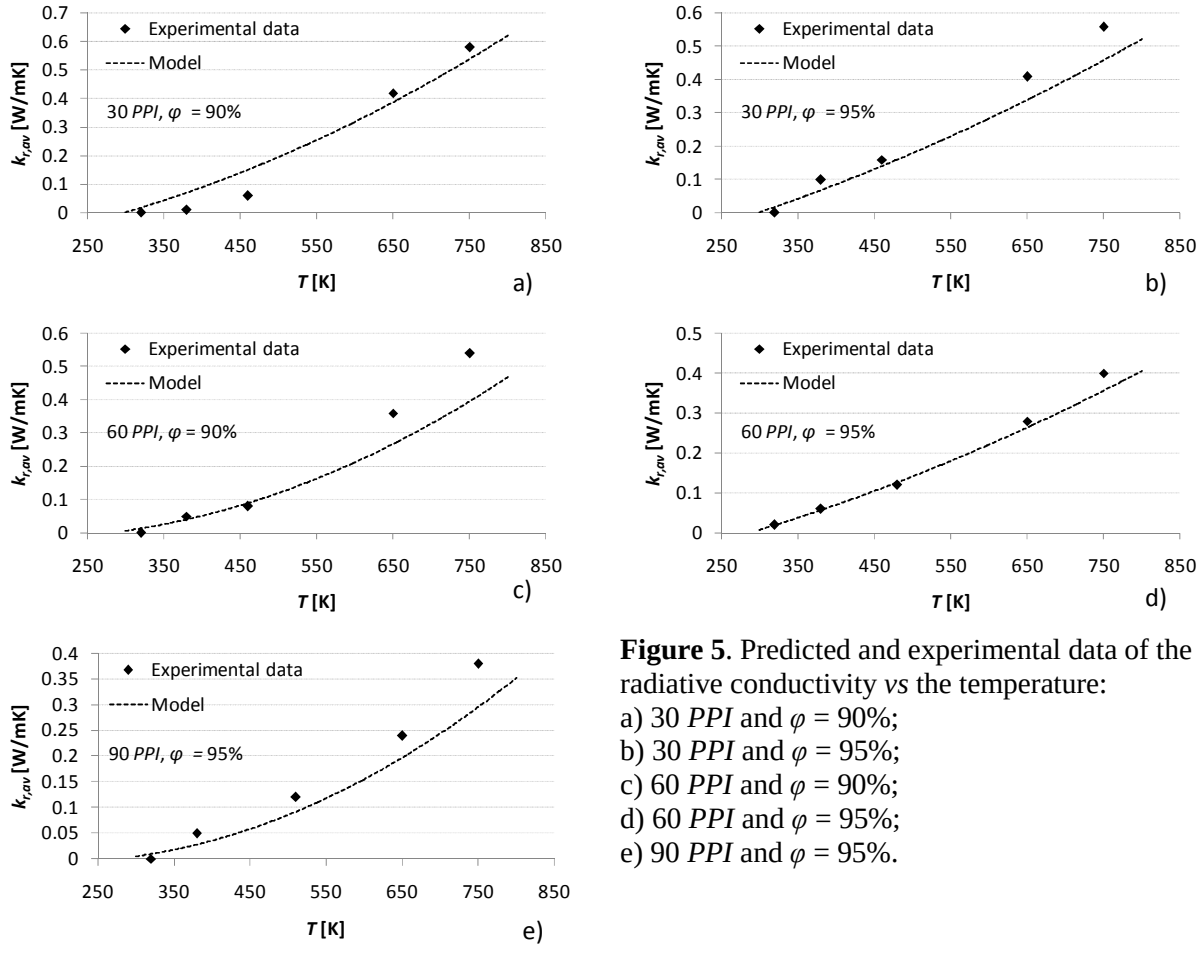

Figure 5. Predicted and experimental data of the radiative conductivity *vs* the temperature:
a) 30 *PPI* and φ = 90%;
b) 30 *PPI* and φ = 95%;
c) 60 *PPI* and φ = 90%;
d) 60 *PPI* and φ = 95%;
e) 90 *PPI* and φ = 95%.

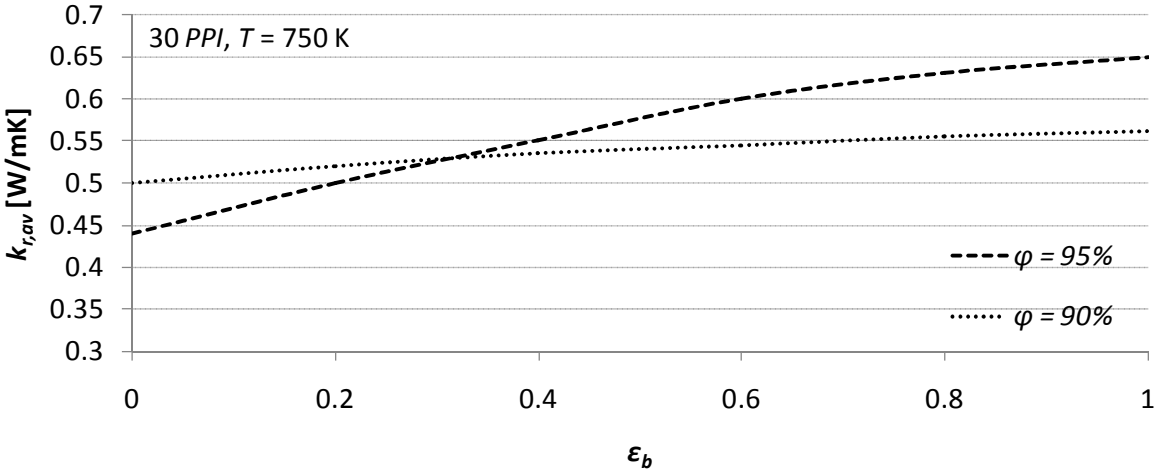

Figure 6. Average radiative conductivity *vs* boundary plates emissivity, for a 30 mm thick sample at T = 750 K, with 30 *PPI*, φ = 90% and φ = 95%.

5. Conclusions

A simplified one-dimensional analytical model of radiative heat transfer in foams is presented. The approach adopted by the model is alternative to the methodology, most frequently used in literature, based on independent scattering from randomly distributed particles and, although in a very simplified fashion, explicitly accounts for the cell-like structure of the foam. The model first reduces the foam to a set of optically equivalent planes and then uses a two-flux like method to model radiation.

Correlations have been proposed to simplify the application of the model, and some examples have been provided, with reference to problems frequently encountered in literature. Finally, the model has been validated comparing its prediction with experimental data from Zhao et al. [16], showing good agreement.

While still based on relatively coarse approximations of the geometric structure of the foam, the proposed model can effectively be used as an alternative analytical reference, with the added advantage of an explicit treatment of radiation energy fluxes and geometry.

6. Nomenclature

A_i	Area of the *i* surface
d_p	Cell diameter
d_0	Ligament diameter
F_{ij}	View factor
I	Irradiation
J	Radiosity
k_r	Radiative conductivity
PPI	Pores Per Inch
q	Heat flux
S_r^n	Volumetric internal energy generation
T	Temperature
y	Cartesian coordinate

Greek symbols

β	Extinction coefficient
β_R	Rosseland mean extinction coefficient
ΔT	Temperature difference
ε	Emissivity
κ	Absorption coefficient
ρ	Reflectivity
σ	Stephan-Boltzmann constant
σ_s	Scattering coefficient
τ	Transmissivity
φ	Porosity

Subscripts

av	Average
b	Boundary plates
eq	Equivalent
in	Incoming
m	Refers to *m*th plane
n	Refers to *n*th plane
net	Net
out	Outgoing
p	Grouped planes
r	Radiative

y	Refers to *y* axis
0	Refers to 0th plane
Superscripts	
m	Refers to *m*th plane
M	Refers to the *M*th plane
n	Refers to *n*th plane
N	Refers to the *N*th plane
0	Refers to 0th plane
∞	Grouping succession limit

7. References

[1] Coquard R, Rochais D and Baillis D, 2012 *Fire technol.* **48.3** 699-732
[2] Zhao C Y 2012, *Int. J. Heat Mass Transfer* **55.13** 3618-32
[3] Glicksmann L R, Schuetz M A and Sinofsky M J 1987 *J. Heat Transfer* **109** 809-12
[4] Kuhn J, Ebert H P, Arduini Schuster M C, Buttner D and Fricke J 1992 *Int. J. Heat Mass Transfer* **35** 1795-1801
[5] Kuhn J, Placido E and Arduini Schuster M C 2005 *Infr. Phys. Technol*. **46** 219-31
[6] Doermann D and Sacadura J F 1996 *J. Heat Transfer* **118** 88-93
[7] Coquard R and Baillis D 2006 *J.Heat Transfer* **128** 538-49
[8] Coquard R, Baillis D and Quenard D 2009 *J. Heat Transfer* **131** 012702.1- 012702.10.
[9] Loretz M, Coquard R, Baillis D and Maire E 2008 *J. Quant. Spectr. Radiat. Transfer* **109** 16-27
[10] Kamiuto K 1997 *JSME Int. J. Series B* **4** 577-82
[11] De Micco C and Aldao C M 2005 *J. Polymer Science B: Polymer Physics* **43.2** 190-2
[12] Zhao C Y, Tassou S A and Lu T J 2008. *Int. J. Heat Mass Transfer* **51** 929-40
[13] Contento G, Oliviero M, Bianco N and Naso V 2014 *J. Thermal Sciences* **76** 147-54
[14] Bhattacharya A, Calmidi V V and Mahajan R L 2002 *Int. J. Heat Mass Transfer* **45.5** 1017-31
[15] Howell J R, Siegel R and Menguc M C 2010 *Thermal Radiation Heat Transfer*, 5th ed., , Taylor and Francis/CRC, New York
[16] Zhao C Y, Lu T J, Hodson H P and Jackson J D 2004 *Mat. Science Eng. A* **367.1** 123-31
[17] Zhao C Y, Kim T, Lu T J and Hodson H P 2001 Micromechanics Centre & Whittle Lab, Department of Engineering, University of Cambridge